Journal of Physics:
Conference Series

Computational Investigation on the Effect of Π-Spacers in Pyrazole-Based Organic Dyes for Dye-Sensitized Solar Cells (DSSCs)

Computational Investigation on the Effect of Π-Spacers in Pyrazole-Based Organic Dyes for Dye-Sensitized Solar Cells (DSSCs)

J. Jasmine Sharmila[a], V. Mohankumar[b], P. Pounraj[c], S. Sundaram[d], A.Umamaheswari[a*]

[a]Department of Physics, Government Arts College, Coimbatore - 641018, Tamil Nadu, India.
[b]Department of Physics, PSG College of Arts & Science, Coimbatore-641014, Tamil Nadu, India.
[c]PG and Research Department of Chemistry, The American College, Tallakulam, Madurai, Tamil Nadu – 625002, India.
[d]Department of Physics, Bannari Amman Institute of Technology, Sathyamangalam, Tamil Nadu 638 401, India.

*Email: aumaphysics305@gmail.com

Abstract. The study explores six donor-π-acceptor organic dye sensitizers (PYQ) derived from 1-hexyl-1H-pyrazole to improve dye-sensitized solar cell (DSSC) performance. To analyse the molecular structures of the dyes theoretical methods including Density Functional Theory (DFT) and Time-Dependent DFT (TDDFT) were utilized. Structural and spectroscopic parameters were optimized using the DFT/B3LYP approach with the 6-311++G(d,p) basis set. The investigation focused on the influence of diverse π-spacers on the functional characteristics of the dyes. Significant parameters including energy levels, electrochemical characteristics, HOMO-LUMO orbitals, injection energy, electronic absorption spectra, light-harvesting efficiency, charge transfer properties, lifetime and dye regeneration energy were assessed. These six dyes exhibit superior characteristics for DSSC applications than the quinoline based parent dyes. PYQ-6 proved the most efficient, compared with other dyes. It demonstrates promising properties such as a low bandgap (2.32 eV), strong oscillator strength (2.516), broad absorption spectrum and high light-harvesting efficiency (0.997).

1. Introduction

Dye-sensitized solar cells (DSSCs) are notable for their simple fabrication process, economic feasibility and eco-friendly nature [1]. DSSC is composed of four main units: the photoanode [2], counter electrode [3], sensitizer [4] and electrolyte [5]. The sensitizer is pivotal in harvesting light by exciting electrons and transferring them into the semiconductor's conduction band [6]. Many researchers have reported that the PCE and electron injection [7] of the dyes may be improved by extending the π-bridge length [8, 9] or by altering the molecular structures of the dyes such as changing the donor or acceptor moieties [10, 11].

Donor-π-Acceptor structured dyes are favored for their tunable structures for targeted properties [12]. Pyrazole-based dyes offer thermal and photostability, strong visible absorption, and active charge transfer, tunable electronic properties [13] and thereby improving light-harvesting efficiency. Their electron-donating nature enhances dye regeneration and reduces recombination losses [14]. The π-bridges are vital in enabling intramolecular charge transfer [15]. Thiophene is a popular choice in DSSCs known for its higher power conversion efficiency (PCE), excellent light absorption [16] and superior charge transport ability [17]. The robust electron-withdrawing nature of cyanovinyl drops the band gap [18] and stabilizes the LUMO level, making it an active π-linker [19]. Quinoline derivatives are preferable for their thermal stability [20] and exceptional optoelectronic properties [21], finding applications in corrosion prevention and electronics [22]. Cyanoacrylic acid is an effective acceptor component because of its strong binding affinity to titanium dioxide surfaces [23]. Theoretical techniques like DFT and TDDFT significantly reduce the cost and time related to the experimental fabrication of novel dyes by identifying suitable sensitizers before synthesis [24]. Through simulations, researchers can study frontier molecular orbitals and gain insights into the electron transfer process [25]. This study highlights the 1-hexyl-1H pyrazole-based (PYQ) sensitizers connected with π-linkers like cyanovinyl, quinoline and thiophene groups along with cyanoacrylic acid functioning as the acceptor group.

This work presents innovative modifications to the π-linkers. It evaluates their influences on the frontier molecular orbitals, absorption spectra, bandgap energies, charge transfer properties and chemical features of the dyes. The findings reveal a clear relationship between the arrangement and distribution of π-spacers, resulting in LUMO stabilization, HOMO destabilization and a notable reduction in the band gap outcomes have not been previously reported.

2. Methods

Every computation in this research was executed by applying the Gaussian 09 W software package [26]. The optimized structures of the PYQ dyes in the gas phase were obtained by employing the B3LYP [27] functional and the 6-311++G (d,p) [28] basis set [29]. To account for the solvent environment (chloroform), the polarizable continuum model (SCRF) [30] was used. Molecular structural images were drawn using the Gauss View 5.0 [31] program package.

2.1. Geometrical structure of the dyes

Figure 1 depicts the π-linker arrangements in six 1-hexyl-1H pyrazole-π-A dye patterns. The 2D representations of synthesized PYQ dyes are shown in Figure 2 and their optimized D-π-A configurations are displayed in Figure 3.

3. Results and Discussion

3.1. Investigation of Frontier Molecular orbitals (FMO)

Understanding how dye sensitizers interact optically requires analysing frontier molecular orbitals (FMO) [32]. Table 1 outlines the HOMO and LUMO energy levels of the PYQ dyes, which possess a systematic trend: the HOMO energy decreases from PYQ-6 to PYQ-1. The LUMO energy decreases from PYQ-1 to PYQ-6. This results in a reduced band gap from PYQ-1 to PYQ-6. Figure 4 presented that PYQ-6 exhibits the lowest bandgap among all the dyes.

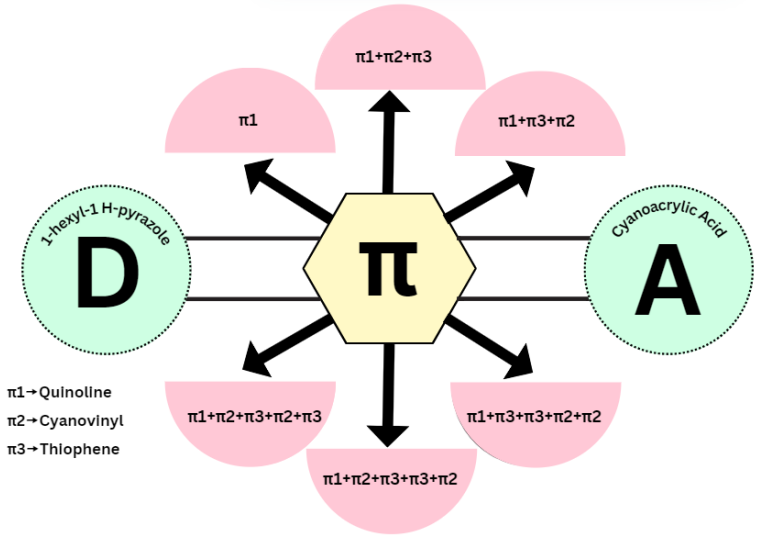

Figure 1. The arrangements of π-linkers of the PYQ dyes

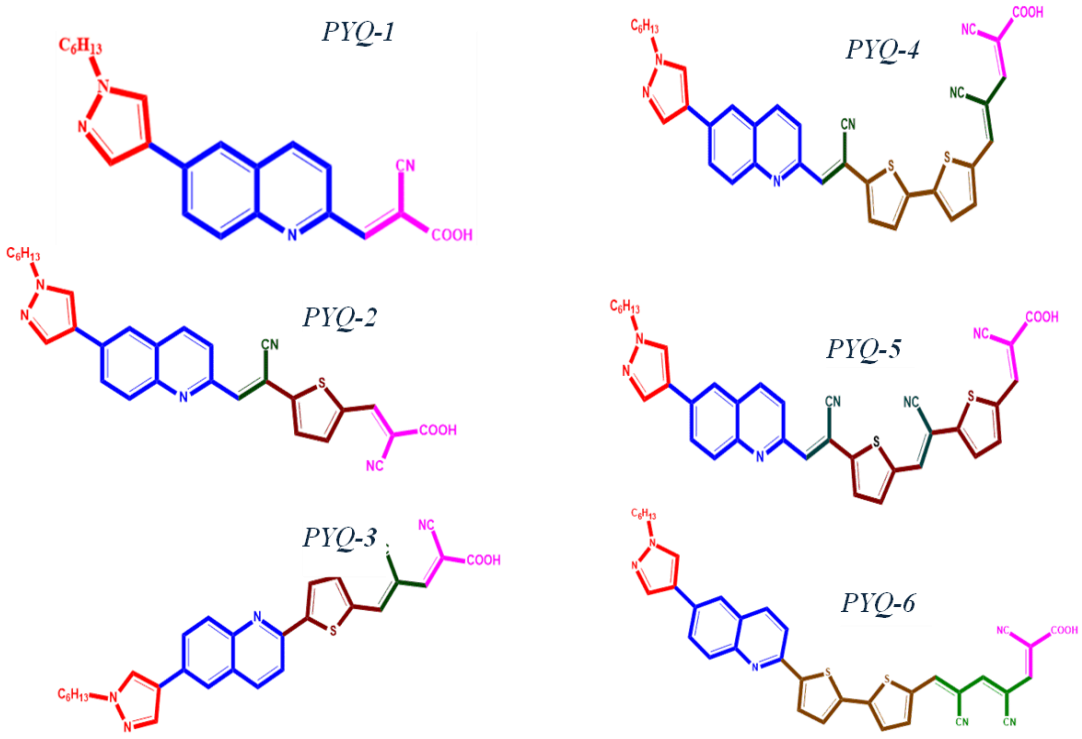

Figure 2. 2D structure of PYQ dyes

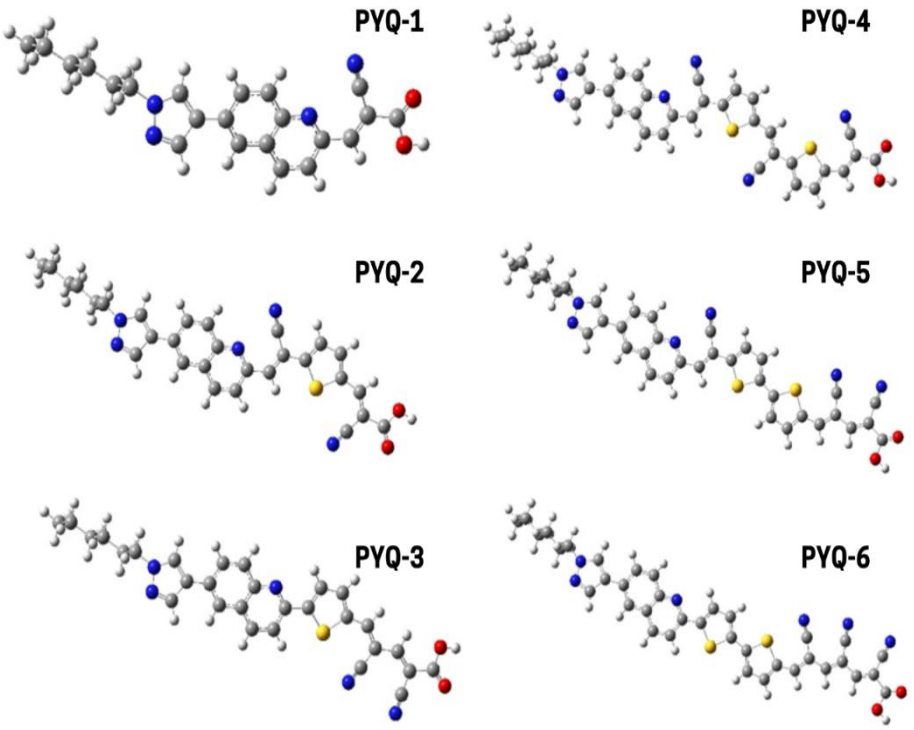

Figure 3. Optimized molecular structure of designed PYQ sensitizers

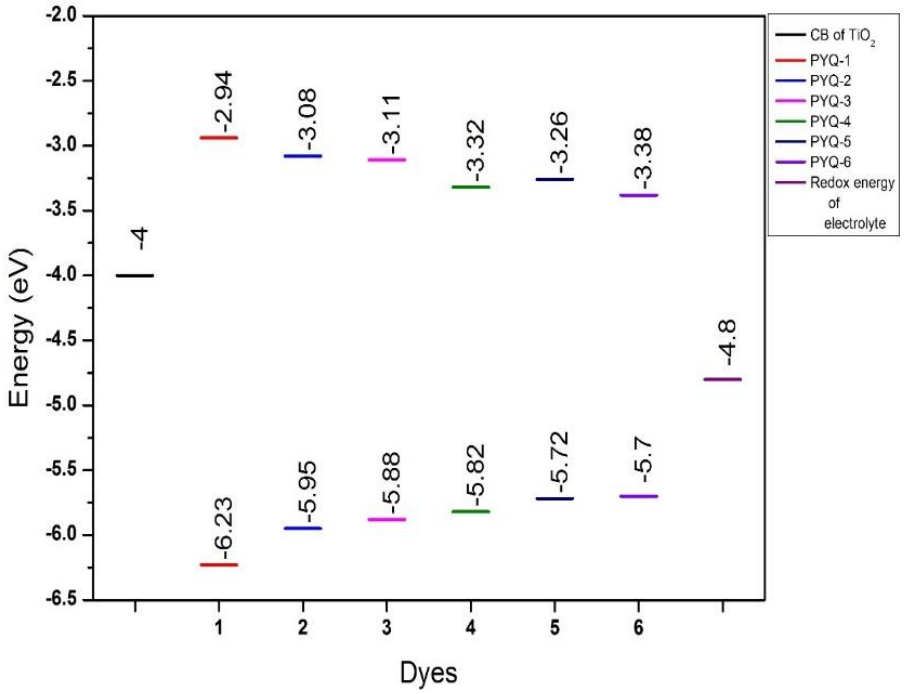

Figure 4. Energy level of PYQ dyes

Table 1. FMO of the PYQ dyes

Dye	HOMO (eV)	LUMO (eV)	Band Gap (eV)
PYQ-1	-6.23	-2.94	3.29
PYQ-2	-5.95	-3.08	2.87
PYQ-3	-5.88	-3.11	2.77
PYQ-4	-5.82	-3.32	2.5
PYQ-5	-5.72	-3.26	2.46
PYQ-6	-5.7	-3.38	2.32

The HOMO is primarily distributed on the 1-hexyl-1H-pyrazole unit and π-linkers with minor contributions in the acceptor region. The π-bridge and the cyanoacrylic group are the key regions of LUMO distribution as illustrated in Figure 5. These orbital distributions are necessary for effective electronic excitation [33] and transition features [34]. The overlapping of HOMO and LUMO orbitals and the construction of a well-separated electronic state boost the effectiveness of electron transfer processes.

3.2.Electronic Absorption Spectrum

TD-DFT approaches can be used to predict the optical properties and electronic absorption spectra of the PYQ dye sensitizers. Table 2 provides the maximum absorption wavelengths λ_{max}. The response of dyes to light influences DSSC efficiency. Modifying spacer units increase λ_{max}, diminishes band gap energy and increases optoelectronic attributes.

The redshift in absorption spectra improves the efficiency of converting light into electrical current [35]. The obtained λ_{max}values of the developed dyes range from 353-506 nm with PYQ-6 showing the highest value. The observed redshift in the PYQ dyes arises from the π-orbital overlap and resonance conjugation [36, 37] as displayed in Figure 6. The electronic absorption spectra span a range of 200–800 nm in the gas phase. It has two bands: the first band spans from 380 to 800 nm and the second band spans from 200 to 380 nm in the gas phase. The absorbance spectrum range for PYQ-1 is 200- 300 nm and 300-450 nm, for PYQ-2 is 200-320 nm and 320-550 nm, for PYQ-3 is 200-320 nm and 320-580 nm, for PYQ-4 is 200-350 nm and 350-700 nm, for PYQ-5 is 200-350 nm and 350-700 nm and for PYQ-6 is 200-350 nm and 350-800 nm. The absorption spectral range in the chloroform phase extend from 200–900 nm confirming sufficient sunlight absorption. In the solvent phase, the absorption peaks exhibit a redshift of 30–50 nm relative to the gas phase.

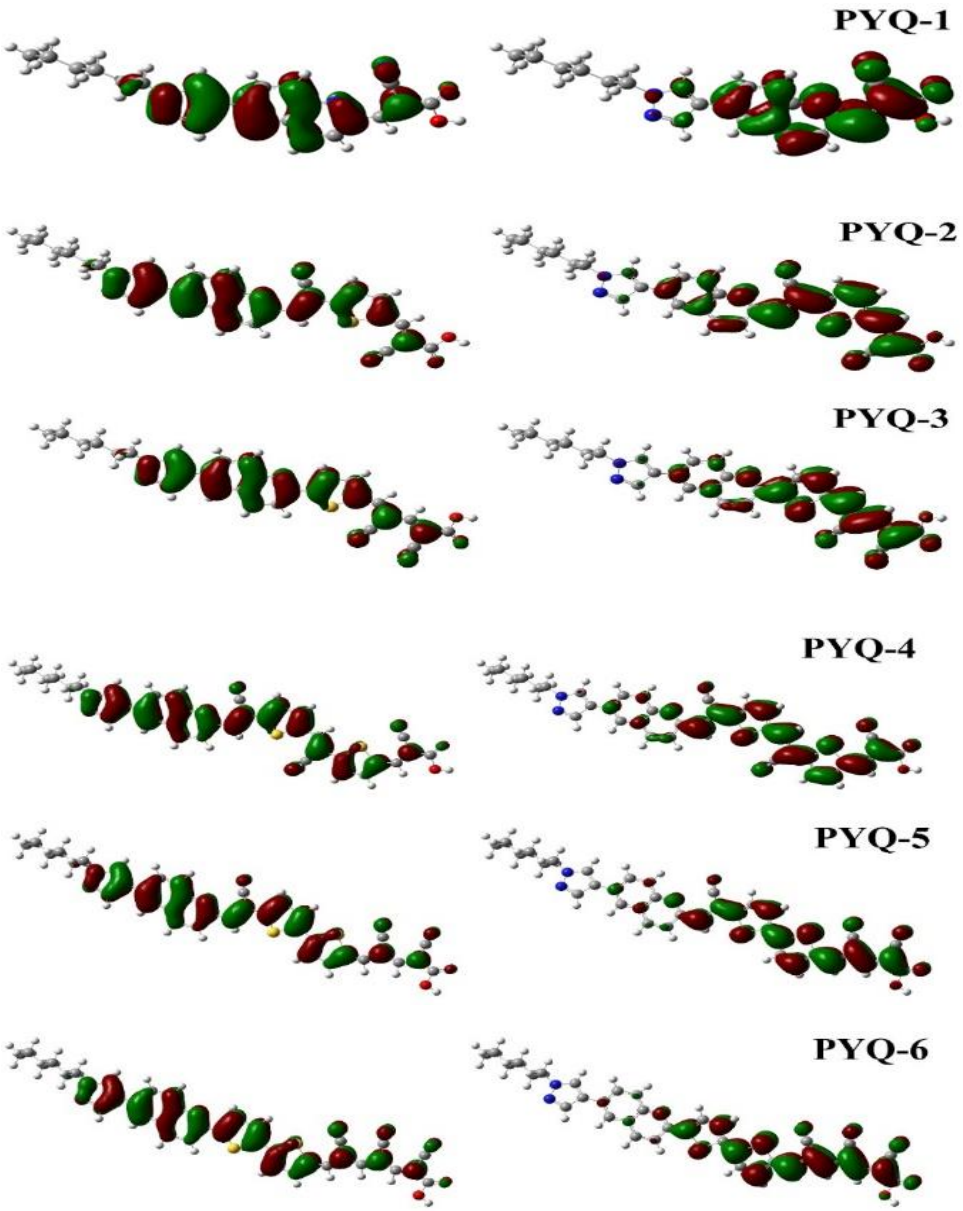

Figure 5. FMO of PYQ sensitizers

Relative to the gas phase, the dyes displayed a broader electronic absorption spectrum in the solvent phase as depicted in Figure 7. In the gas phase, λ_{max}values of the dyes are ranked as follows: PYQ-6 > PYQ-5 = PYQ-4 > PYQ-2 > PYQ-3 > PYQ-1. The broader absorption region and higher λ_{max} value of PYQ-6 compared to the other dyes highlight PYQ-6 as the most efficient dye sensitizer.

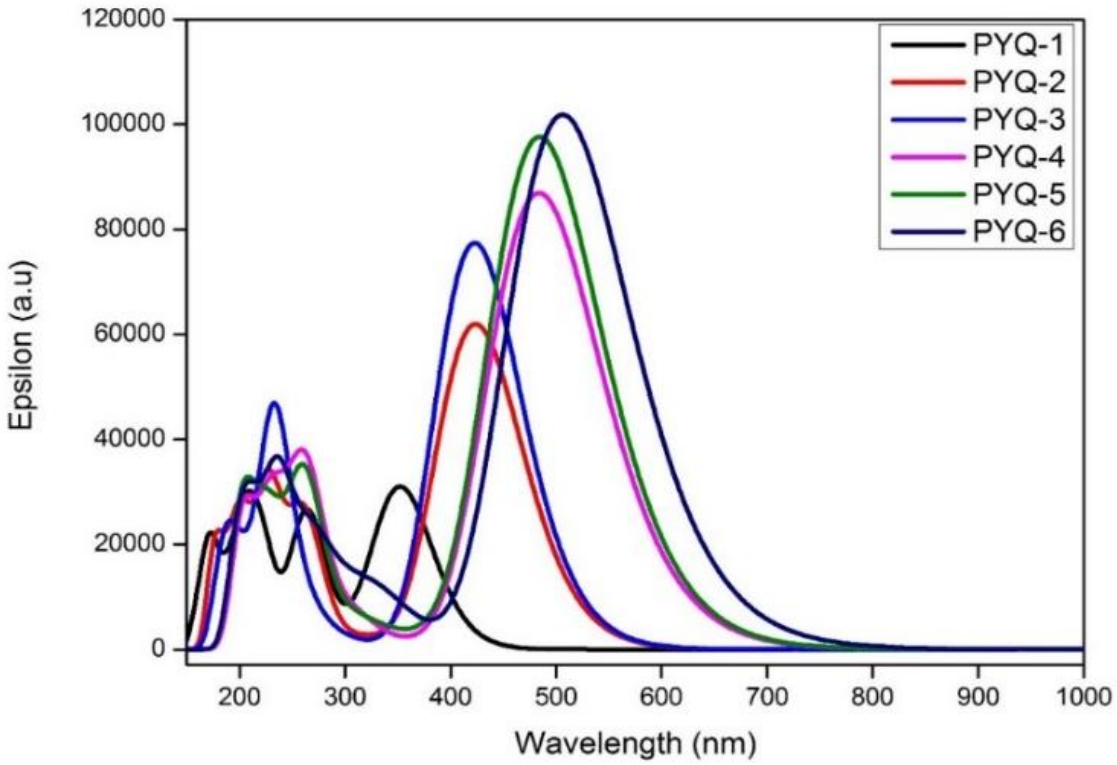

Figure 6. Electronic absorption spectrum of PYQ dyes in the gas phase

Table 2. The excited state parameters of the dyes

Dyes	Energy (eV)	Wave length Maximum λ_{max} (nm)	Contribution		Oscillator Strength (f)	LHE
			Major	Minor		
PYQ-1	3.51	353	H→L (91%)	H-3→L (4%), H-1→L+1 (2%), H→L+1 (2%)	0.7517	0.823
PYQ-2	2.93	424	H-1→L (11%), H→L (82%)	H-1→L+1 (2%), H→L+1 (3%)	1.5300	0.971
PYQ-3	2.93	423	H-1→L (11%), H→L (83%)	H→L+1 (2%)	1.9121	0.988
PYQ-4	2.56	484	H→L (81%)	H-1→L (9%), H-1→L+1 (3%)	2.1470	0.993
PYQ-5	2.56	484	H-1→L (11%), H→L (79%)	H-1→L+1 (2%), H→L+1 (3%)	2.4109	0.996
PYQ-6	2.45	506	H-1→L (10%), H→L (82%)	H→L+1 (3%)	2.5157	0.997

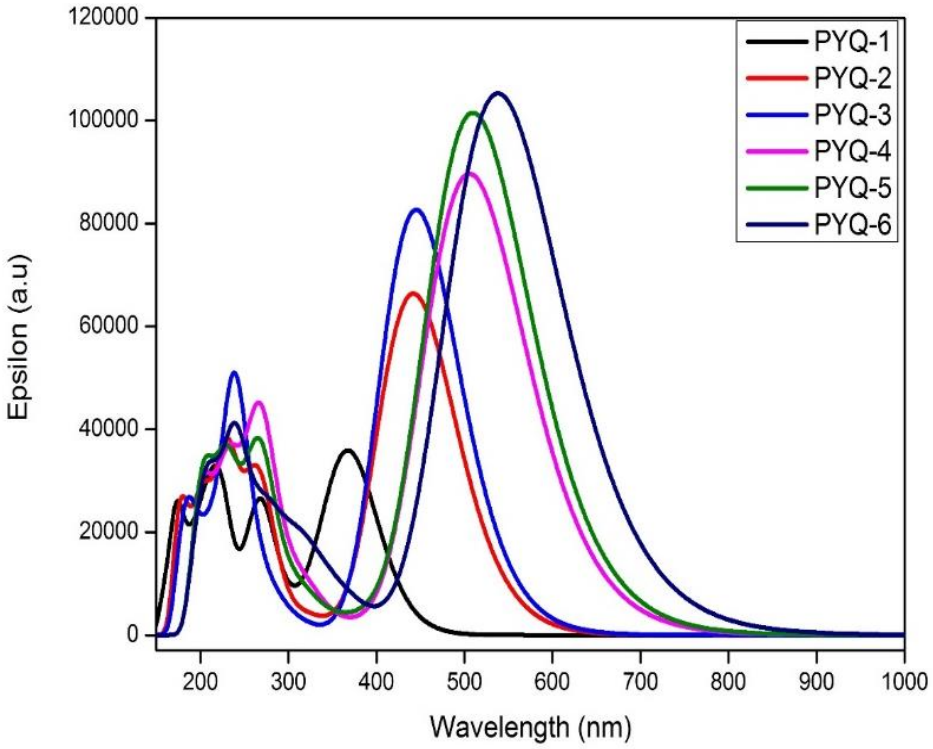

Figure 7. Electronic absorption spectrum of PYQ dyes in the solvent phase

3.3.The Light harvesting efficiency (LHE)

The LHE was determined using the equation $LHE = 1 - 10^{-f}$ [38] in which f corresponds to the oscillator strength at the peak wavelength [39]. The LHE values estimated between 0.823 and 0.997 and rank the dyes in the order PYQ-6>PYQ-5>PYQ-4>PYQ-3>PYQ-2>PYQ-1 which confirms that PYQ6 exhibits superior performance among the dyes.

3.4. Charge transfer properties

The electron injection efficiency represents the ratio of excited electrons from the dye that reach the semiconductor's conduction band plays a vital step in producing electricity [40]. The LUMOs of the dyes are positioned above the energy level of the conduction band edge, enabling efficient charge injection [41]. ΔG_{inject} and ΔG_{dye}^{regen} values are calculated using the formula 1,2,3 [42].

$$\Delta G_{inject} = E_{ox}^{dye*} - E_{CB}^{SC} \quad (1)$$

$$E_{OX}^{dye*} = E_{ox}^{dye} - E(\lambda_{max}) \quad (2)$$

$$\Delta G_{dye}^{regen} = E_{ox}^{dye} - E_{red}^{electrolyte} \quad (3)$$

Where, E_{ox}^{dye} -Redox potential of the iodide/triiodide electrolyte, E_{ox}^{dye*}-Oxidized potential in the excited state, ΔG_{inject}- driving force of electron injection, ΔG_{regen}- driving force of regeneration. The E_{OX}^{dye}, E($\lambda_{\max}^{ICT}$), E_{OX}^{dye*}, ΔG^{inject} and G_{dye}^{regen} for 6 dyes were computed by TD-DFT and listed in Table 3. Here the redox potential of the iodide/triiodide electrolyte is equal

to 4.8 eV [43] and E_{CB}^{SC} is -4.0 eV [44]. Minimized ΔG_{regen}values reduce the recombination and thereby decreasing the dye degradation [45]. The estimated negative values of ΔG^{inject} represent that the sensitizers undergo spontaneous processes for both dye regeneration and the charge injection [46]. Adequate driving force is necessary for dye regeneration and minimizing further electron loss [47]. A higher ΔG_{regen} value of all the created dyes boosts their inherent ability to absorb electrons.

Table 3. Photovoltaic attributes of the PYQ dyes

Dye	ΔE (eV)	E_{ox}^{dye} (eV)	E_{ox}^{dye*} (eV)	ΔG_{inject} (eV)	ΔG_{regen} (eV)	V_{OC} (eV)
PYQ-1	3.51	6.23	2.72	-1.28	1.43	1.06
PYQ-2	2.93	5.95	3.02	-0.98	1.15	0.92
PYQ-3	2.93	5.88	2.95	-1.05	1.08	0.89
PYQ-4	2.56	5.82	3.26	-0.74	1.02	0.68
PYQ-5	2.56	5.72	3.16	-0.84	0.92	0.74
PYQ-6	2.45	5.7	3.25	-0.75	0.9	0.62

3.5. The open-circuit voltage (V_{OC})

The open-circuit voltage is a critical parameter in photovoltaic performance and influences the effectiveness of DSSCs [48]. A higher $\boldsymbol{V_{OC}}$ indicates a stronger electron injection ability, and is closely tied to the maximum theoretical efficiency of the cell [49]. Factors such as light intensity, energy levels of compounds, solar cell temperature, charge carrier recombination, the electrode's work function, fluorescence efficiency and material composition all play crucial roles in calculating $\boldsymbol{V_{OC}}$ [50]. The $\boldsymbol{V_{OC}}$ can be estimated by the energy difference between E_{LUMO} and E_{CB} of titanium dioxide and this relationship is given by the following equation 4 [51]

$$V_{OC} = E_{LUMO} - E_{CB} \quad (4)$$

The derived $\boldsymbol{V_{OC}}$ values fall within the range of 0.62 to 1.06 eV. All $\boldsymbol{V_{OC}}$ values are positive, indicating sufficient feasibility for efficient electron transfer. Consequently, the designed dyes exhibit strong potential as effective dye-sensitizers for DSSC applications.

3.6. Radiative lifetime (τ)

The radiative lifetime of dyes is essential in determining their light-emitting efficiency, which is significant for boosting optoelectronic features [52]. A longer radiative lifetime indicates better efficiency, diminishes the rate of charge recombination and makes it a required characteristic in dye design [53]. Prolonging the radiative lifetime promotes electron transition from the 1-hexyl-1H-pyrazole part's LUMO to the cyanoacrylic acid unit's LUMO [54]. The

radiative lifetime (τ) depends on the inverse of the oscillator strength and the square of the transition energy and is given by the relation $\tau = 1.499/fE^2$ [55]. The lifetime of PYQ dyes are displayed in Table 4 and is obtained within the range of 1.484 ns to 2.488 ns. The radiative lifetime of the created PYQ dyes is in the following pattern: PYQ-1> PYQ-2> PYQ-4> PYQ-6>PYQ-5>PYQ-3. These τ values support ideal parameters for minimizing the possibility of radiative recombination [56].

Table 4. Radiative lifetime (τ in ns) of the PYQ dyes

Dyes	Energy (cm^{-1})	Oscillator strength (f)	Life time (τ) (ns)
PYQ-1	28310	0.7517	2.488
PYQ-2	23632	1.5300	1.754
PYQ-3	23632	1.9121	1.404
PYQ-4	20648	2.1470	1.638
PYQ-5	20648	2.4109	1.458
PYQ-6	19761	2.5157	1.526

3.7. Chemical parameters

The chemical characteristics are determined by applying the formulas 5-14 [57] and presented in Table 5.

Ionization potential $IP = -HOMO$ (5)

Electron affinity $EA = -LUMO$ (6)

Chemical potential $\mu = -\frac{1}{2}(IP + EA)$ (7)

Chemical hardness $\eta = \frac{1}{2}(IP - EA)$ (8)

Electronegativity $\chi = \frac{IP+EA}{2}$ (9)

Electrophilicity index $\omega = \frac{\mu^2}{\eta}$ (10)

Electron donating power $\omega^+ = \frac{(IP+3EA)^2}{16(IP-EA)}$ (11)

Electron accepting power $\omega^- = \frac{(3IP+EA)^2}{16(IP-EA)}$ (12)

Maximum electronic charge transfer $\Delta N_{max} = \frac{-\mu}{\eta}$ (13)

Softness $S = \frac{1}{2\eta}$ (14)

The chemical potential values indicate the readiness of the dyes to enable electron transfer and hardness (η) provides insights into the molecule's stability and transport reactivity [58]. The hardness (η) which is the inverse of softness (S) assesses the molecular stability and reactivity

[59]. The lower chemical hardness (η) of PYQ dyes suggests a strong capacity to contribute electrons to TiO_2.

Table 5. Chemical features of the dyes

Dye	PYQ-1	PYQ-2	PYQ-3	PYQ-4	PYQ-5	PYQ-6
Ionization Potential (IP) (eV)	6.23	5.95	5.88	5.82	5.72	5.70
Electron affinity (EA) (eV)	2.94	3.08	3.11	3.32	3.26	3.38
Chemical potential (μ) (eV)	-4.585	-4.515	-4.495	-4.570	-4.490	-4.540
Chemical hardness (η) (eV)	1.645	1.435	1.385	1.250	1.230	1.160
Softness (S) (eV)	0.304	0.348	0.361	0.400	0.407	0.431
Electronegativity (χ) (eV)	4.585	4.515	4.495	4.570	4.490	4.540
Electrophilicity index (ω) (eV)	12.780	14.206	14.589	16.708	16.390	17.769
Electron donating power ($\boldsymbol{\omega^-}$) (eV)	8.888	9.540	9.715	10.795	10.594	11.299
Electron accepting power ($\boldsymbol{\omega^+}$) (eV)	4.303	5.025	5.220	6.225	6.104	6.759
*E*lectronic charge transfer $\boldsymbol{\Delta N_{max}}$	2.787	3.146	3.246	3.656	3.650	3.914

The chemical reactivity is strongly associated with the chemical potential defined as the rate of energy change with the number of electrons and is equivalent to the negative of electronegativity [60]. The higher electronegativity values PYQ dyes support its ability to attract electrons effectively and strengthen the bonding with the semiconductor surface.

The electron donating power (ω^-) denotes the ability of the molecule to contribute electrons, while electron accepting power (ω^+) represents its capacity to receive electrons [61]. A lower ω^- indicates a more efficient electron donor, while a higher ω^+ indicates a more powerful electron acceptor. The calculated ω^- and ω^+ values range from 8.888 eV to 11.299 eV and 4.303 eV to 6.759 eV respectively. The ω^+ and ω^- values were improved by the addition and specific position of π-spacers within the dye structure. All the PYQ dyes are having higher electrophilicity index (ω) and maximum electronic charge transfer ΔN_{max}values [62], which exhibit remarkable potential as electrophiles and enrich their ability to absorb electronic charge [63]. The electrophilicity index (ω) reflects a molecule's tendency to attract electrons and its stabilization energy when gaining electrons from the surroundings [64]. The ω values for the

dyes follow this order: PYQ6->PYQ4->PYQ-5>PYQ-3>PYQ-2>PYQ-1. PYQ-6 is the strongest electrophile among the dyes and is highly effective for optoelectronic applications.

3.8. Natural Bond Orbital Analysis (NBO)

Natural Bond Orbital (NBO) analysis is an essential tool for understanding charge transfer [65] and assessing intramolecular and intermolecular interactions [66]. Table 6 illustrates the NBO charges of PYQ dyes.

Table 6. NBO charges of PYQ dyes

Dye	q^D	q^π	q^A	Δq^{D-A}
PYQ-1	0.0552	0.01545	-0.07068	0.12588
PYQ-2	0.05479	0.08126	-0.13606	0.19085
PYQ-3	0.05077	0.21637	-0.26711	0.31788
PYQ-4	0.05394	0.08603	-0.1399	0.19384
PYQ-5	0.05182	0.03669	-0.08849	0.14031
PYQ-6	0.04653	0.03272	-0.07925	0.12578

The net charge populations of the PYQ dyes were evaluated by NBO analysis [67] with the donor, π-linker and acceptor charges symbolized as q^D , q^π and q^A respectively. The charge difference between the donor and acceptor is expressed as Δq^{D-A}. The results suggest that all molecules possess positive charges on the donor (1-hexyl-1H pyrazole) and π-spacer components. The acceptor unit exhibits a concentration of negative charges while the positive charges found on the π-bridge imply its donor behaviour. The most negative NBO charge in all the dyes is consistently found on the acceptor unit affirming its role as the most powerful electron acceptor.

4. Conclusion

Using DFT/TDDFT computations, the photoelectric properties of six D-π-A dye sensitizers for DSSCs in the gas phase were explored. Structural alterations were achieved by incorporating π-spacers such as quinoline/cyanovinyl/thiophene that exhibit the best optical features, tunable band gaps and advanced charge transfer efficiency. These π- linkers trigger the intramolecular charge transfer from 1-hexyl-1H pyrazole to the acceptor part. The FMO analysis revealed that the designed dyes reduce the energy gap and enrich the absorption characters leading to a red shift in the absorption peaks. The higher LHE supports better conversion of energy and intramolecular charge transfer. The less positive ΔG_{regen} values and the negative ΔG_{inject} values of all the dyes indicate desirable electron injection. The absorption spectrum in the chloroform phase is wider than in the gas phase with remarkable peak intensities. PYQ-6 emerges as the most efficient sensitizer for DSSCs, offering the lowest band gap (2.32 eV), the highest light harvesting efficiency (0.997), a wide absorption spectrum and exceptional overall performance.

Acknowledgments
The authors V. Mohankumar and P. Pounraj reveal their gratitude to Prof. P. Ramasamy, Dean, (Research), SSN Institutions, Chennai.

References

[1] Ren Z, Cao Y, Shang C and Sun C 2022 Chemical Physics Letters 806 140035.
[2] Govindaraj R, Santhosh N, Pandian M S and Ramasamy P 2017 Journal of Crystal Growth 468 125-128.
[3] Vijayakumar P, Pandian M S, Pandikumar A and Ramasamy P, 2017 Materials Science and Engineering 222 7-17.
[4] Robertson N 2006 45(15) 2338-2345.
[5] Meng Q B, Takahashi K, Zhang X T, Sutanto I, Rao T N, Sato O, Fujishima A, Watanabe H, Nakamori T and Uragami M 2003 19(9) 3572-3574.
[6] Haid S, Marszalek M, Mishra A, Wielopolski M, Teuscher J, Moser J E, Humphry-Baker R, Zakeeruddin S M, Grätzel M and Bäuerle P 2012 Advanced Functional Materials 22(6) 1291-1302.
[7] Sivanadanam J, Mukkamala R, Mandal S, Vedarajan R, Matsumi N, Aidhen I S and Ramanujam K 2018 international journal of hydrogen energy 43(9) 4691-4705.
[8] Noh H J, Ji J M, Hwang S P, Kim C H and Kim H K 2021 Dyes and Pigments 195 109681.
[9] Heng P, Mao L, Guo X, Wang L and Zhang J 2020 Journal of Materials Chemistry C 8(7) 2388-2399.
[10] Li H, Koh T.M, Hao Y, Zhou F, Abe Y, Su H, Hagfeldt A, Grimsdale A C 2014 Chem Sus Chem 7(12) 3396–3406.
[11] Ganesan P, Yella A, Holcombe T W, Gao P, Rajalingam R, Al-Muhtaseb S A, Grätzel M and Nazeeruddin M K 2015 ACS Sustainable Chemistry & Engineering 3(10) 2389-2396.
[12] Mishra A, Fischer M K and Bäuerle P 2009 Angewandte Chemie International Edition 48(14) 2474-2499.
[13] Farag A M and Fahim A M 2019 Journal of Molecular Structure 1179 304-314.
[14] John A M, Thomas R, Balakrishnan S P, Al-Zaqri N, Alsalme A and Warad I 2021 Zeitschrift für Physikalische Chemie 235(9)1227-1245.
[15] Devadiga D, Selvakumar N, Shetty P, Sridhar Santosh M, Chandrabose R S and Karazhanov S 2021 International Journal of Energy Research 45 6584.
[16] Wills K A, Mandujano-Ramírez H J, Merino G, Oskam G, Cowper P, Jones M D, Cameron P J and Lewis S E 2016 Dyes and Pigments 134 419-426.
[17] Cornil J, Dos Santos D A, Beljonne D and Brédas J L 1995 The Journal of Physical Chemistry 99(15) 5604-5611.
[18] Manoharan S and Anandan S 2014 Dyes and Pigments 105 223-231.
[19] Xu M, Zhang M, Pastore M, Li R, De Angelis F and Wang P 2012 Chemical Science 3(4) 976-983.
[20] Dos Santos G C, Oliveira E F, Lavarda F C and da Silva-Filho L C 2019 Journal of molecular modeling 25 1-13.
[21] Slodek A, Matussek M, Filapek M, Szafraniec-Gorol G, Szlapa A, Grudzka-Flak I, Szczurek M, Malecki J G, Maron A, Schab-Balcerzak E and Nowak E M 2016 European Journal of Organic Chemistry 2016(14) 2500-2508.
[22] Park S R, Seo J S, Ahn Y, Lee J H and Suh M C 2018 Organic Electronics 63 194-199.
[23] Park K W, Serrano L A, Ahn S, Baek M H, Wiles A A, Cooke G and Hong J 2017 Tetrahedron 73(8) 1098-1104.

[24] Souilah M, Hachi M, Fitri A, Benjelloun A T, El Khattabi S, Benzakour M, Mcharfi M and Zgou H 2021 Research on Chemical Intermediates 47(2) 875-893.
[25] Deogratias G, Seriani N, Pogrebnaya T and Pogrebnoi A 2020 Journal of Molecular Graphics and Modelling 94 107480.
[26] Frisch M J, Trucks G W et. al 2009 Inc, Wallingford CT 201.
[27] Becke A D, 1988 Physical review A 38(6) 3098.
[28] Petersson A, Bennett A, Tensfeldt T G, Al-Laham M A, Shirley W A and Mantzaris J 1988 The Journal of chemical physics 89(4) 2193-2218.
[29] Walsh P J, Gordon K C et. el 2006 Computational Theoretical Chemistry 759 17-24 .
[30] Scalmani G and Frisch M J 2010 The Journal of chemical physics 132(11).
[31] Dennington R, Keith T and Millam J 2009 GaussView Version 5 Semichem Inc Shawnee Mission KS.
[32] Wang T H, Wang I T, Huang W L and Huang L Y 2014 Spectrochimica Acta Part A: Molecular and Biomolecular Spectroscopy 121 650-656.
[33] Ramkumar S and Manidurai P 2017 Spectrochimica Acta Part A: Molecular and Biomolecular Spectroscopy 173 425-431.
[34] Rezvani M, Ganji M D, Jameh-Bozorghi S and Niazi A 2018 Spectrochimica Acta Part A: Molecular and Biomolecular Spectroscopy 194 57-66.
[35] Gunawardhana P, Balasooriya Y, Kandanapitiye M S, Chau Y F C, Kooh M R R and Thotagamuge R 2023 Applied Sciences 14(1) 188.
[36] Cherrak K, Khamaysa O M A, Bidi H, El Massaoudi M, Ali I A, Radi S, El Ouadi Y, El-Hajjaji F, Zarrouk A and Dafali A 2022 Journal of Molecular Structure 1261 132925.
[37] Fatima K, Pandith A.H, Manzoor T and Qureashi A 2023 ACS omega 8(9) 8865-8875.
[38] Khan M U, Anwar A, Hassan A U, Alshehri S M and Sohail A 2024 Energy Science & Engineering 12(9) 3681-3703.
[39] Jasmine Sharmila J, Mohankumar V, Pounraj P, Sundaram S and Umamaheswari A, 2024 Int. Res. J. Multi discip. Tech 6(6) 292-302.
[40] Vuai S A H, Khalfa M S and Babu N S 2024 Chemistry Open 13 e202300307.
[41] Daeneke T, Mozer A J, Uemura Y, Makuta S, Fekete M, Tachibana Y, Koumura N, Bach U and Spiccia L 2012 Journal of the American Chemical Society 134(41) 16925-16928.
[42] Ouared I and Rekis M 2021 Comput. Theor. Chem. 1202 113247.
[43] Fitri A, Benjelloun A.T, Benzakour M, Mcharfi, M, Hamidi M and Bouachrine M 2014 Spectrochimica Acta Part A: Molecular and Biomolecular Spectroscopy 124 646-654.
[44] Conradie J 2023 Journal of Molecular Graphics and Modelling 121 108459.
[45] Tripathi A, Ganjoo A and Chetti P 2020 Solar Energy 209 194-205.
[46] Kacimi R, Raftani M, Abram T, Azaid A, Ziyat H, Bejjit L, Bennani M N and Bouachrine M 2021 Heliyon 7(6).
[47] Panneerselvam M, Kathiravan A, Solomon R V and Jaccob M 2017 Physical Chemistry Chemical Physics 19(8) 6153-6163.
[48] Vuai S.A, Khalfan M S and Babu N S 2021 Heliyon 7(11).
[49] Borbón S, Lugo S, Pourjafari D, Pineda Aguilar N, Oskam G and López I 2020 ACS omega 5(19) 10977-10986.
[50] Ma W, Jiao Y and Meng S 2014 The Journal of Physical Chemistry C 118(30) 16447-16457.
[51] Verma P and Chetti P 2025 Chemical Physics Impact 10 100789.

[52] Ren P, Sun C, Shi Y, Song P, Yang Y and Li Y 2019 Journal of Materials Chemistry C 7(7) 1934-1947.
[53] Tommalieh M J, Aljameel A I, Hussein R K, Al-Heuseen K, Alghamdi S K and Alrub S A 2024 International Journal of Molecular Sciences 25(13) 7138.
[54] Bourouina A and Rekis M 2021 Journal of Molecular Modeling 27(8) 225.
[55] Mohankumar V, Pounraj P, Pandian M S and Ramasamy P 2019 Journal of Molecular Structure 1195 494-505.
[56] Li M, Kou L, Diao L, Zhang Q, Li Z, Wu Q, Lu W, Pan D and Wei Z 2015 The Journal of Physical Chemistry C 119(18) 9782-9790.
[57] Pounraj P, Ramasamy P and Pandian M S 2021 Journal of Molecular Graphics and Modelling 102 107779.
[58] Delgado-Montiel T, Baldenebro-López J, Soto-Rojo R and Glossman-Mitnik D 2020 Molecules 25(16) 3670.
[59] O'boyle N M, Tenderholt A L and Langner K M 2008 Journal of computational chemistry 29(5) 839-845.
[60] Mathiyalagan A, Manimaran K, Muthu K and Rajakantham M 2021 Results in Chemistry 3 100164.
[61] Delgado-Montiel T, Soto-Rojo R, Baldenebro-López J and Glossman-Mitnik D 2019 Molecules 24(21) 3897.
[62] Chattaraj P K, Sarkar U and Roy D R 2006 Chem. Rev. 106 2065–2091.
[63] Domingo L R, Ríos-Gutiérrez M and Pérez P 2016 Molecules 21(6) 748.
[64] Afolabi S O, Semire B and Idowu M A 2021 Heliyon 7(4).
[65] Rajan V K and Muraleedharan K 2017 Food chemistry 220 93-99.
[66] Tseng C Y, Taufany F, Nachimuthu S, Jiang J C and Liaw D J 2014 Organic Electronics 15(6) 1205-1214.
[67] Mohankumar V, Pounraj P, Pandian M S and Ramasamy P 2021 Journal of Molecular Modeling 27(6) 151.